ELectronics EXpress

LETTER

IEICE Electronics Express, Vol.11, No.23, 1–11

A fast in-situ SINS and Doppler sensor calibration algorithm for underwater vehicle navigation

Li Kang, Lingyun Ye[a)], and Kaichen Song

College of Biomedical Engineering & Instrument Science, Zhejiang University, Hangzhou, Zhejiang, 310027, China

a) *lyye@zju.edu.cn*

Abstract: This paper reports the development and experimental evaluation of an in-situ calibration algorithm of the misalignment mounting angle matrix between the Strapdown inertial navigation system (SINS) and Doppler sensor which are practically used for accurate underwater navigation. Most previously reported methods required the SINS to be aligned first to output accurate attitude before the calibration. By separately treating the body frame and the navigation frame attitude update, the algorithm in this paper could be simultaneously carried out during the SINS attitude alignment stage. Simulation and experiment results show that the calibration could be done in 300 s and the position error during the navigation is less than 0.8% of the voyage distance.

Keywords: Doppler navigation, inertial navigation, calibration algorithm, attitude update

Classification: Electronic instrumentation and control

References

[1] P. G. Savage: *Strapdown Analytics* (Strapdown Associates, Maple Plain, 2000) 1-1.

[2] D. Titterton and J. Weston: *Strapdown Inertial Navigation Technology* (The American Institute of Aeronautics and Astronautics, Reston, 2004) 2nd ed. 2.

[3] B. Jalving, K. Gade, K. Svartveit, A. Willumsen and R. Sorhagen: Modeling Identification and Control **25** (2004) 223. DOI:10.4173/mic.2004.4.2

[4] P. M. Lee, B. H. Jeon, S. M. Kim, H. T. Choi, C. M. Lee, T. Aoki and T. Hyakudome: OCEANS'04. MTTS/IEEE TECHNO-OCEAN'04 (2004) 1586. DOI:10.1109/OCEANS.2004.1406359

[5] L. Stutters, H. H. Liu, C. Tillman and D. J. Brown: IEEE Trans. Syst. Man Cybern. C **38** (2008) 581. DOI:10.1109/TSMCC.2008.919147

[6] O. Hegrenaes and E. Berglund: OCEANS 2009-EUROPE (2009) 1. DOI:10.1109/OCEANSE.2009.5278307

[7] J. Young, F. Rowe, B. Brumley and S. Bradley: Proc. of the 1998 Workshop on Autonomous Underwater Vehicles (1998) 89. DOI:10.1109/AUV.1998.744444

[8] K. H. Tang, J. L. Wang, W. L. Li and W. Q. Wu: Sensors **13** (2013) 14583. DOI:10.3390/s131114583

[9] Z. Lv, K. Tang and M. Wu: 2011 10th International Conference on Electronic

DOI: 10.1587/elex.11.20140994
Received October 17, 2014
Accepted November 7, 2014
Publicized November 21, 2014
Copyedited December 10, 2014

Measurement & Instruments (ICEMI) (2011) 336. DOI:10.1109/ICEMI.2011.6037829
[10] J. C. Kinsey and L. L. Whitcomb: IEEE Trans. Robot. **23** (2007) 124. DOI:10.1109/TRO.2006.886829
[11] R. Pollard and J. Read: J. Atmos. Ocean. Technol. **6** (1989) 859. DOI:10.1175/1520-0426(1989)006<0859:AMFCSA>2.0.CO;2
[12] T. M. Joyce: J. Atmos. Ocean. Technol. **6** (1989) 169. DOI:10.1175/1520-0426(1989)006<0169:OISOSA>2.0.CO;2
[13] J. C. Kinsey and L. L. Whitcomb: IEEE J. Oceanic Eng. **32** (2007) 286. DOI:10.1109/JOE.2007.893686
[14] P. G. Savage: J. Guid. Control Dyn. **21** (1998) 19. DOI:10.2514/2.4228
[15] Y. Wu and X. Pan: IEEE Trans. Aerosp. Electron. Syst. **49** (2013) 1006. DOI:10.1109/TAES.2013.6494395
[16] D. W. Eggert, A. Lorusso and R. B. Fisher: Mach. Vis. Appl. **9** (1997) 272. DOI:10.1007/s001380050048
[17] H. S. Hong, J. G. Lee and C. G. Park: IEE Proc., Radar Sonar Navig. **151** (2004) 57. DOI:10.1049/ip-rsn:20030698

1 Introduction

SINS is a self-contained navigation system which could continuously provide position, velocity, and attitude information based on the vehicle's angular rate and linear acceleration measured by an Inertial Measurement Unit (IMU) [1, 2]. For the feature of self-contained and continuity of navigation information, the SINS becomes a key navigation equipment for the underwater vehicles' navigation [3, 4, 5, 6]. However, owing to the drift of the IMU measurements, a single SINS cannot afford precise position and velocity for a long period of time without any aiding methods. Doppler Velocity Log (DVL) which could offer accurate body frame velocity based on Doppler shift is the most commonly used aiding source [7]. However there are always mounting angles between the SINS's body frame and the DVL's body frame. The accuracy of DVL/INS integration will be reduced owing to these mounting angles.

So, it is necessary to calibrate and compensate these mounting angles before a navigation mission is operated. The common method is to transfer the position or velocity information gathered from an aiding source such as Global Navigation Satellite System (GNSS) into the SINS's body frame according to the attitude. After voyaging a certain distance, an enough signal noise ratio (SNR) between the travel distance and the position error could be obtained [8]. And the mounting angles between the SINS and DVL could be estimated through a Kalman filter [9] or a least square error estimator [10]. The vertical position can be directly gathered from a pressure sensor while the horizontal positions must be integrated from the velocity. So, earlier works placed more emphasis on the vertical mounting angle since this angle error produced the most horizontal velocity errors [11, 12]. Another reason of only the vertical mounting angle is treated is the low SNR of the vertical position channel since the vertical travel distance on the surface is small. With a more precise position sensor as long-baseline (LBL) is introduced, Kinsey [13] et al. improved the calibration accuracy and three dimensional mounting angle errors were estimated.

DOI: 10.1587/elex.11.20140994
Received October 17, 2014
Accepted November 7, 2014
Publicized November 21, 2014
Copyedited December 10, 2014

IEICE Electronics Express, Vol.11, No.23, 1–11

However, all these methods require the SINS to be aligned first to provide accurate attitude information before the calibration. And the calibration's accuracy depends on the aligned attitude. Practically, the attitude errors of each alignment are different according to the bias drift of the gyroscopes. Besides, the mounting angles may be slightly changed between two missions. So it is better to calibrate the mounting angles before each navigation mission. This paper based on the analysis of the attitude update equation to propose a fast in-situ SINS and Doppler sensors calibration algorithm which could be simultaneously carried out in the alignment stage of the SINS. It means that the calibration does not require additional time. The rest of the paper is organized as follows. Section 2 explains the problem in mathematics. Section 3 proposes the calibration algorithm by separately treating the body frame and the navigation frame attitude update. The performance of the algorithm is evaluated with simulation in Section 4 and on-lake test in Section 5. Conclusions are drawn in Section 6.

2 Problem statement

Defining e the Earth frame, i the nonrotating inertial frame, n the local level navigation frame with east-north-up geodetic axes, b the strapdown inertial sensors' body frame, d the DVL's body frame, n' the n frame with some errors, b' the b frame with some errors. The DVL's velocity could be transferred into the n frame through the following equation as

$$\mathbf{v}^n(t) = \mathbf{C}_{b(t)}^{n(t)}\mathbf{C}_d^b\mathbf{v}^d(t) \tag{1}$$

where $\mathbf{v}^d(t)$ is the DVL's velocity output, $\mathbf{C}_d^b$ is the mounting angle DCM which should be estimated, $\mathbf{C}_{b(t)}^{n(t)}$ is the attitude direction cosine matrix (DCM) from the b frame to the n frame tracked by the SINS, it could be updated through the following equation as [14]

$$\dot{\mathbf{C}}_b^n = \mathbf{C}_b^n\omega_{nb}^b\times \tag{2}$$

where ω_{nb}^b is the angular rate of the SINS in the b frame with respect to the n frame defined as [14]

$$\omega_{nb}^b = \omega_{ib}^b - \mathbf{C}_n^b\left(\omega_{ie}^n + \omega_{en}^n\right) \tag{3}$$

ω_{ib}^b is the angular rate measured by the gyroscopes in the b frame, ω_{ie}^n is the angular rate of the Earth's rotation in the n frame, ω_{en}^n is the rotation angular rate of the n frame with respect to the e frame, $(\cdot)\times$ is a skew symmetric matrix form of a cross-product which satisfies $\mathbf{a}\times\mathbf{b} = (\mathbf{a}\times)\ \mathbf{b}$.

Practically, owing to the gyroscopes' errors, we could only get the attitude DCM's approach as $\mathbf{C}_b^{n'}$. And since the mounting angle of each mission may be changed, we could only get the mounting angle DCM's approach as $\mathbf{C}_d^{b'}$ before the calibration. So Eq. (1) should be modified as

$$\mathbf{v}^n(t) = \mathbf{C}_{n'}^n\mathbf{C}_{b(t)}^{n'(t)}\mathbf{C}_{b'}^b\mathbf{C}_d^{b'}\mathbf{v}^d(t) \tag{4}$$

where $\mathbf{C}_{n'}^n$ is the misalignment attitude DCM and $\mathbf{C}_{b'}^b$ is the misalignment mounting angle DCM. The angles contained in $\mathbf{C}_{n'}^n$ and $\mathbf{C}_{b'}^b$ are all small angles, so the sequence of $\mathbf{C}_{n'}^n$ and $\mathbf{C}_{b'}^b$ in Eq. (4) can be swapped as

DOI: 10.1587/elex.11.20140994
Received October 17, 2014
Accepted November 7, 2014
Publicized November 21, 2014
Copyedited December 10, 2014

$$\mathbf{v}^n(t) = \mathbf{C}_{b(t)}^{n'(t)}\mathbf{C}_{n'}^{n}\mathbf{C}_{b'}^{b}\mathbf{C}_{d}^{b'}\mathbf{v}^d(t) \tag{5}$$

Since a roughly known mounting angle DCM could be obtained from previous calibration, the goal is to estimate the DCM defined as

$$\mathbf{C}_{fix} = \mathbf{C}_{n'}^{n}\mathbf{C}_{b'}^{b} \tag{6}$$

during the SINS's alignment stage that $\mathbf{C}_{b(t)}^{n'(t)}$ is inaccurate.

3 Calibration algorithm

Eq. (2) is the traditional attitude update equation. Nowadays, the attitude update can be separately treated based on the DCM product chain rule as [14]

$$\mathbf{C}_{b(t+\Delta t)}^{n(t+\Delta t)} = \mathbf{C}_{n(t)}^{n(t+\Delta t)}\mathbf{C}_{b(t)}^{n(t)}\mathbf{C}_{b(t+\Delta t)}^{b(t)} \tag{7}$$

The update method for $\mathbf{C}_{n(t)}^{n(t+\Delta t)}$ and $\mathbf{C}_{b(t+\Delta t)}^{b(t)}$ is also proposed in [14]. If this rule is applied in each update cycle, the attitude update equation can be written as

$$\mathbf{C}_{b(t)}^{n(t)} = \mathbf{C}_{n(0)}^{n(t)}\mathbf{C}_{b(0)}^{n(0)}\mathbf{C}_{b(t)}^{b(0)} \tag{8}$$

The update equation for $\mathbf{C}_{n(t)}^{n(0)}$ and $\mathbf{C}_{b(t)}^{b(0)}$ [15] are

$$\dot{\mathbf{C}}_{n(t)}^{n(0)} = \mathbf{C}_{n(t)}^{n(0)}(\omega_{ie}^{n} + \omega_{en}^{n})\times = \mathbf{C}_{n(t)}^{n(0)}\omega_{in}^{n}\times \tag{9}$$

$$\dot{\mathbf{C}}_{b(t)}^{b(0)} = \mathbf{C}_{b(t)}^{b(0)}\omega_{ib}^{b}\times \tag{10}$$

Substituting Eq. (6) and (8) into Eq. (5) yields

$$\mathbf{C}_{n(0)}^{b(0)}\mathbf{C}_{n(t)}^{n(0)}\mathbf{v}^n(t) = \mathbf{C}_{b(t)}^{b(0)}\mathbf{C}_{fix}\mathbf{v}^{b'}(t) \tag{11}$$

According to Eq. (6), $\mathbf{C}_{fix}$ is a small angle DCM. So the sequence of Eq. (11) can be changed as

$$\mathbf{C}_{n(0)}^{b(0)}\mathbf{C}_{n(t)}^{n(0)}\mathbf{v}^n(t) = \mathbf{C}_{fix}\mathbf{C}_{b(t)}^{b(0)}\mathbf{v}^{b'}(t) \tag{12}$$

To utilize the GNSS position estimate, both sides of Eq. (12) can be integrated to acquire

$$\alpha(t) = \mathbf{C}_{fix}\beta(t) \tag{13}$$

where

$$\alpha(t) = \int_0^t \mathbf{C}_{n(0)}^{b(0)}\mathbf{C}_{n(\tau)}^{n(0)}\mathbf{v}^n(\tau)d\tau \tag{14}$$

$$\beta(t) = \int_0^t \mathbf{C}_{b(\tau)}^{b(0)}\mathbf{v}^{b'}(\tau)d\tau \tag{15}$$

For the equation like (13), $\mathbf{C}_{fix}$ can be uniquely solved by an optimization method using the singular value decomposition (SVD) [16] as

Step 1: Calculate a 3×3 matrix as

$$\mathbf{H} = \sum_{n=1}^{t/T}\beta(nT)\alpha(nT)^T \tag{16}$$

Step 2: Determine the SVD of $\mathbf{H}$

$$\mathbf{H} = \mathbf{USV}^T \tag{17}$$

DOI: 10.1587/elex.11.20140994
Received October 17, 2014
Accepted November 7, 2014
Publicized November 21, 2014
Copyedited December 10, 2014

IEICE Electronics Express, Vol.11, No.23, 1–11

Step 3: Calculate $\mathbf{C}_{fix}$

$$\mathbf{C}_{fix} = \begin{cases} \mathbf{V}\mathbf{U}^T & if \ \ \det(\mathbf{H}) \geq 0 \\ \mathbf{V} \cdot diag(1, 1, -1) \cdot \mathbf{U}^T & if \ \ \det(\mathbf{H}) < 0 \end{cases} \tag{18}$$

So the key is how to calculate $\alpha(t)$ and $\beta(t)$.

$\alpha(t)$ is developed as

$$\begin{aligned} \alpha(t) &= \int_0^t \mathbf{C}_{n(0)}^{b(0)} \mathbf{C}_{n(\tau)}^{n(0)} \mathbf{v}^n(\tau) d\tau = \mathbf{C}_{n(0)}^{b(0)} \int_0^t \mathbf{C}_{n(\tau)}^{n(0)} \dot{p}^n(\tau) d\tau \\ &= \mathbf{C}_{n(0)}^{b(0)} \left[\mathbf{C}_{n(\tau)}^{n(0)} p^n(\tau)|_0^t - \int_0^t \dot{\mathbf{C}}_{n(\tau)}^{n(0)} p^n(\tau) d\tau \right] \end{aligned} \tag{19}$$

Applying Eq. (9) into the integration part of Eq. (19) yields

$$\begin{aligned} &\int_0^t \dot{\mathbf{C}}_{n(\tau)}^{n(0)} \mathbf{p}^n(\tau) d\tau = \int_0^t \mathbf{C}_{n(\tau)}^{n(0)} \omega_{in}^n \times \mathbf{p}^n(\tau) d\tau \\ &= \sum_{k=0}^{M-1} \mathbf{C}_{n(t_k)}^{n(0)} \left[\left(\tfrac{T}{2} \mathbf{I} + \tfrac{T^2}{6} \omega_{in}^n \times \right) \omega_{in}^n \times \mathbf{p}^n(t_k) + \left(\tfrac{T}{2} \mathbf{I} + \tfrac{T^2}{3} \omega_{in}^n \times \right) \omega_{in}^n \times \mathbf{p}^n \left(t_{k+1} \right) \right] \end{aligned} \tag{20}$$

The derivation of Eq. (20) is similar with [15]. Then

$$\begin{aligned} \alpha(t) = \mathbf{C}_{n(0)}^{b(0)} \Bigg\{ &\mathbf{C}_{n(\tau)}^{n(0)} p^n(\tau)|_0^t \\ &- \sum_{k=0}^{M-1} \mathbf{C}_{n(t_k)}^{n(0)} \left[\left(\tfrac{T}{2} \mathbf{I} + \tfrac{T^2}{6} \omega_{in}^n \times \right) \omega_{in}^n \times \mathbf{p}^n(t_k) + \left(\tfrac{T}{2} \mathbf{I} + \tfrac{T^2}{3} \omega_{in}^n \times \right) \omega_{in}^n \times \mathbf{p}^n \left(t_{k+1} \right) \right] \Bigg\} \end{aligned} \tag{21}$$

The calculation method for $\beta(t)$ is also similar in [15] as

$$\beta(t) = \int_0^t \mathbf{C}_{b(\tau)}^{b(0)} \mathbf{v}^{b'}(\tau) dt = \sum_{k=0}^{M-1} \mathbf{C}_{b(t_k)}^{b(0)} \int_{t_k}^{t_{k+1}} \mathbf{C}_{b(t)}^{b(t_k)} \mathbf{v}^{b'}(\tau) dt \tag{22}$$

where

$$\begin{aligned} &\int_{t_k}^{t_{k+1}} \mathbf{C}_{b(t)}^{b(t_k)} \mathbf{v}^{b'}(\tau) dt \approx \int_{t_k}^{t_{k+1}} \left(\mathbf{I} + \left(\int_{t_k}^{t} \omega_{ib}^b d\tau \right) \times \right) \mathbf{v}^{b'}(\tau) dt \\ &= \Delta\mathbf{p}_1 + \Delta\mathbf{p}_2 + \tfrac{1}{2} (\Delta\theta_1 + \Delta\theta_2) \times \left(\Delta\mathbf{p}_1 + \Delta\mathbf{p}_2 \right) + \tfrac{2}{3} \left(\Delta\theta_1 \times \Delta\mathbf{p}_2 + \Delta\mathbf{p}_1 \times \Delta\theta_2 \right) \end{aligned} \tag{23}$$

$\Delta\mathbf{p}_1$, $\Delta\mathbf{p}_2$, $\Delta\theta_1$, and $\Delta\theta_2$ are the incremental position and angle described as

$$\begin{aligned} \Delta\mathbf{p}_1 &= \int_0^{T/2} \mathbf{v}^{b'} \, dt \\ \Delta\mathbf{p}_1 + \Delta\mathbf{p}_2 &= \int_0^{T} \mathbf{v}^{b'} \, dt \end{aligned} \tag{24}$$

$$\begin{aligned} \Delta\theta_1 &= \int_0^{T/2} \omega_{ib}^b dt \\ \Delta\theta_1 + \Delta\theta_2 &= \int_0^{T} \omega_{ib}^b dt \end{aligned} \tag{25}$$

For $\alpha(t)$ and $\beta(t)$, all the parameters can be computed during the SINS's attitude alignment stage except $\mathbf{C}_{b(0)}^{n(0)}$. It means that the algorithm does not need back tracking if $\mathbf{C}_{b(0)}^{n(0)}$ could be obtained. $\mathbf{C}_{b(t)}^{n(t)}$ is gradually approaching its true value during this stage [17]. And a reasonable $\mathbf{C}_{b(t)}^{n(t)}$ could be obtained when the alignment is finished. It takes about 300 s for a navigation grade SINS to finish the in-motion attitude alignment. 300 s is enough for the calibration. So, $\mathbf{C}_{b(0)}^{n(0)}$ could be achieved according to the inverse of Eq. (8) as

DOI: 10.1587/elex.11.20140994
Received October 17, 2014
Accepted November 7, 2014
Publicized November 21, 2014
Copyedited December 10, 2014

ELectronics EXpress
IEICE Electronics Express, Vol.11, No.23, 1–11

$$\mathbf{C}_{b(0)}^{n(0)} = \mathbf{C}_{n(t)}^{n(0)}\mathbf{C}_{b(t)}^{n(t)}\mathbf{C}_{b(0)}^{b(t)} \tag{26}$$

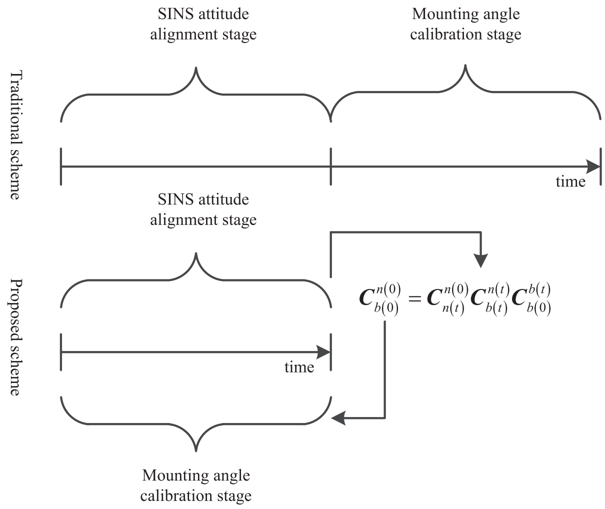

Fig. 1. Scheme of the calibration algorithm.

Fig. 1 shows the scheme of the calibration algorithm. With the new calibration algorithm, the misalignment mounting angle could be gathered when $\mathbf{C}_{b(0)}^{n(0)}$ is obtained. So the mounting angle calibration stage does not need additional time.

4 Simulation results

Two simulations are carried out in this section to examine the performance of the calibration algorithms.

The simulations' base latitude is 30 deg. The pitch, roll, and heading are sinusoid waves with random magnitude and frequency within 10 deg and 1 Hz. The trajectory is a line with random velocity around 1 m/s. The trajectory is on the surface, so the vertical channel performances a ±1 m vibration within 1 Hz.

The first simulation lasts for 300 s. Error free sensors are used in the first simulation. Misalignment mounting angles and misalignment attitude are added to the simulation. Table I and Table II show the estimate and compensation results.

Since the misalignment mounting angles are small, Table I only shows the condition of less than 6 deg. It is clear that the misalignment mounting angles could

Table I. Estimate and compensation results of misalignment mounting angles

Misalignment mounting angles (deg)						Position errors (m)	
x		y		z			
ideal	estimate error	ideal	estimate error	ideal	estimate error	Before compen-sation	After compen-sation
0	0.004	0	0.008	0	0.006	0.07	0.005
0.5	0.011	0.5	0.047	0.5	0.002	6	0.17
1	0.028	1	0.105	1	0.002	12	0.35
3	0.121	3	0.348	3	0.009	36	1.1
6	0.325	6	0.745	6	0.010	73	2.1

DOI: 10.1587/elex.11.20140994
Received October 17, 2014
Accepted November 7, 2014
Publicized November 21, 2014
Copyedited December 10, 2014

be estimated. The residual errors are only about 10% of the original errors, and 97% of the position errors are compensated. For a navigation grade SINS, the heading error should be smaller than 2 deg, the pitch and roll errors are about tenth of the heading error. So Table II only gives the results that the heading errors are less than 6 deg. The results are similar to Table I.

Table II. Estimate and compensation results of SINS misalignment attitude angles

SINS misalignment attitude angles (deg)						Position errors (m)	
pitch		roll		heading			
ideal	estimate error	ideal	estimate error	ideal	estimate error	Before compensation	After compensation
0	0.004	0	0.008	0	0.006	0.07	0.005
0.05	0.008	0.05	0.018	0.5	0.022	5	0.12
0.1	0.011	0.1	0.037	1	0.025	11	0.25
0.3	0.014	0.3	0.122	3	0.042	33	0.74
0.6	0.013	0.6	0.275	6	0.063	67.1	1.44

The second simulation imitates the attitude alignment stage and navigation stage of a SINS. Sensor errors are considered in the second simulation. They are gyroscopes drift: within 0.2 deg/h, gyroscopes noise: 0.9 deg/h/$\sqrt{\text{Hz}}$, accelerometers bias: within 1×10^{-4} g, accelerometers noise: 2×10^{-4} g/$\sqrt{\text{Hz}}$, DVL long term error: 1.5% of voyage velocity, DVL noise: standard variance 0.02 m/s, GNSS position accuracy: ±3 m. And misaligned mounting angle errors are random values within 1.5 deg.

For the first 300 s, a GNSS aided in-motion alignment [17] is carried out. The mounting angle calibration process is also presented in this stage. Then, navigation is processed to evaluate the calibration effect. The simulation runs 100 times. Fig. 2 demonstrates the average navigation errors.

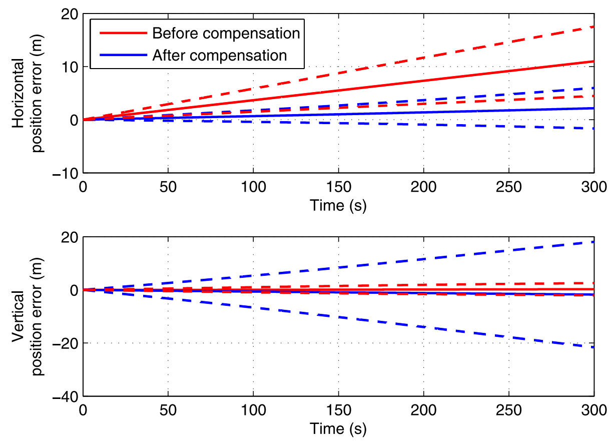

Fig. 2. Average navigation errors before and after the mounting angle error calibration. Dashed lines are its 1σ envelop.

Before compensation, the horizontal position error reaches 11.0 ± 6.5 m when the vehicle travels 300 s (about 300 m). It equals to 3.6 ± 2.2% of voyage distance.

DOI: 10.1587/elex.11.20140994
Received October 17, 2014
Accepted November 7, 2014
Publicized November 21, 2014
Copyedited December 10, 2014

IEICE Electronics Express, Vol.11, No.23, 1–11

While after compensation, the horizontal position error is 2.1 ± 3.8 m which equals to $0.7 \pm 1.3\%$ of voyage distance. It is at least 2 times better than the uncompensated condition.

While for the vertical channel, the results are bad. This is because the SNR of the vertical channel is low since the vehicle is traveling on the surface. There are few travel distance. In order to prove it, we add a vertical motion to the simulation. The vertical motion's speed is about 0.35 m/s. And the results are displayed in Fig. 3. With vertical motion added, the errors of the vertical channel are significantly decreased from -1.8 ± 19.8 m to -1.3 ± 3.8 m. And the horizontal position errors are also decreased from 2.1 ± 3.8 to 1.6 ± 0.9 m.

It is clear from the simulation results that a higher accuracy needs high SNR in both horizontal and vertical channels. So the best way for the mounting angle calibration/SINS attitude alignment is to use a positioning sensor such as LBL which could provide position information underwater. Otherwise, the vertical channel's position errors would be large. Practically the vertical channel's position can also be gathered from a pressure sensor. It is acceptable to use a GNSS as an aiding sensor since the horizontal position errors are still small. So only a GPS was used in the experiment in the next section.

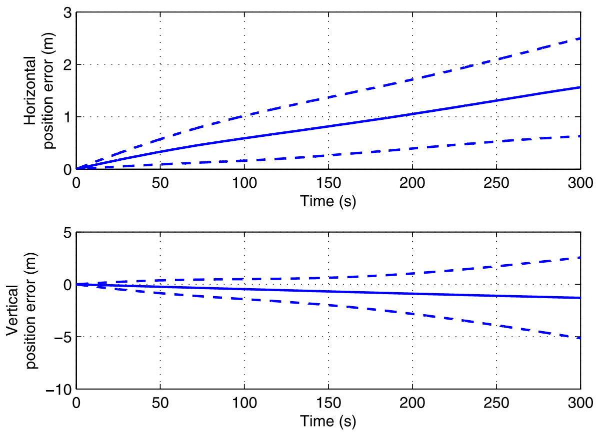

Fig. 3. Average navigation errors after vertical motion added. Dashed lines are its 1σ envelop.

5 Experimental results

The calibration experiment data was collected in the Thousand Islands Lake in Zhejiang Province. The sensors used for the experiment are listed as

1) SINS: The IMU contains four fiber optics gyroscopes (bias instability: 0.2 deg/h) and four quartz accelerometers (bias: 1×10^{-4} g). The sensor sample rate is 100 Hz.
2) DVL: Long term accuracy: 1.5% of the voyage distance. The original data output rate is 4–5 Hz.
3) GPS: Position accuracy: 3 m. The data output rate is 5 Hz. The GPS is used as an aiding sensor during the SINS attitude alignment/mounting angle calibration stage and a standard during the navigation stage for the results comparison.

DOI: 10.1587/elex.11.20140994
Received October 17, 2014
Accepted November 7, 2014
Publicized November 21, 2014
Copyedited December 10, 2014

IEICE Electronics Express, Vol.11, No.23, 1–11

Fig. 4 shows the experiment setup. The GPS is installed on the top of the vehicle, and the SINS and DVL are fixed under water. A roughly known mounting angle DCM $\mathbf{C}_d^{b'}$ was already obtained according to the mechanical structure design. The vehicle's voyage velocity is around 1 m/s during the experiment.

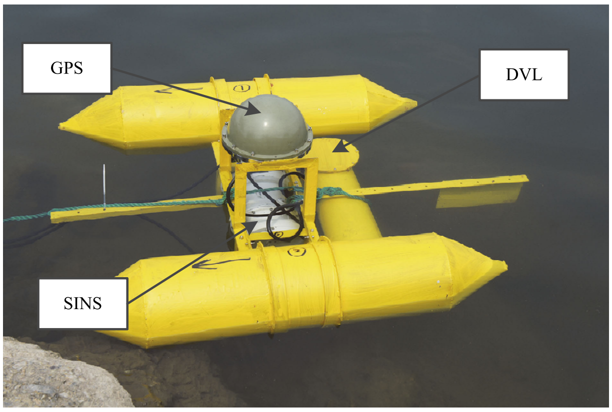

Fig. 4. Experiment setup with a SINS, a DVL, and a GPS.

The trajectory of the vehicle is displayed in Fig. 5. Two calibrations were done in the whole voyage. Each calibration includes a 300 s mounting angle calibration stage (the blue and red dashed lines) and a 1200 s navigation stage (the blue and red solid lines). A GPS aided SINS attitude alignment [17] is also done during the mounting angle calibration stage. And during the navigation stage, the GPS signals are blocked to the navigation system to evaluate the performance of the DVL aided navigation after calibration. Besides, Calibration 1 also includes a comparison between the new algorithm and a traditional algorithm proposed in [10]. The traditional algorithm needs additional attitude alignment time. In order to make the start point of each calibration algorithm the same, this alignment is carried out before the calibration shown in the green dashed lines. It means that the traditional algorithm requires more time before the navigation system could enter the normal navigation mode.

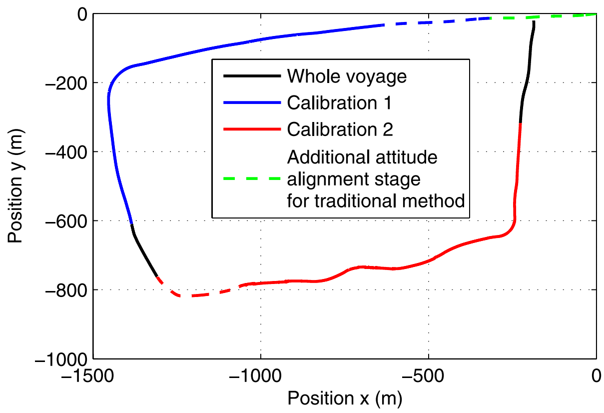

Fig. 5. The route of the vehicle.

DOI: 10.1587/elex.11.20140994
Received October 17, 2014
Accepted November 7, 2014
Publicized November 21, 2014
Copyedited December 10, 2014

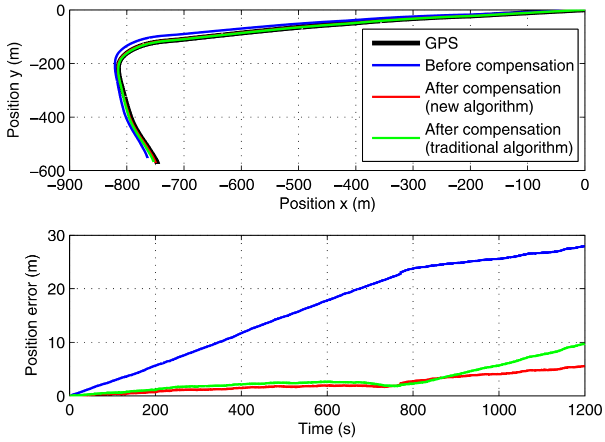

Fig. 6. Navigation results of the first calibration.

Table III. Statistics of the first calibration

	Position error (m) Max	Position error (m) Average	Position error /voyage distance	Time before navigation (s)
Before compensation	27.9	16.4	2.3%	300
After compensation (new algorithm)	5.5	2.3	0.5%	300
After compensation (traditional algorithm)	9.7	3.1	0.8%	600

Fig. 6 and Table III demonstrate the navigation results of the first calibration. The final position error is 27.9 m before compensation. And the error after compensation is 5.5 m for the new algorithm and 9.7 m for the traditional algorithm which equals to 0.5% and 0.8% of the voyage distance. The results show that both the new algorithm and the traditional algorithm could effectively complete the calibration and compensation task, while the new algorithm could save much time since the new algorithm can be simultaneously carried out during the attitude alignment stage.

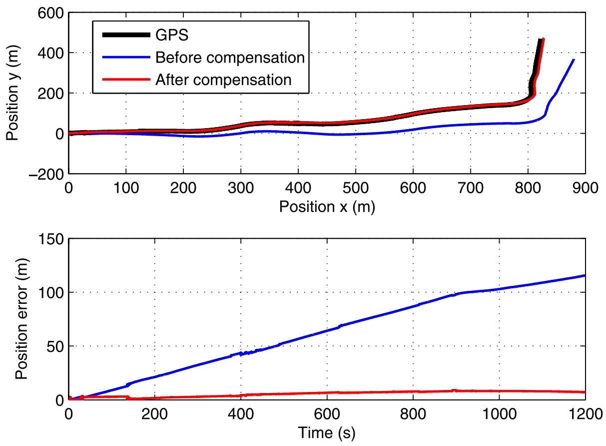

Fig. 7. Navigation results of the second calibration.

DOI: 10.1587/elex.11.20140994
Received October 17, 2014
Accepted November 7, 2014
Publicized November 21, 2014
Copyedited December 10, 2014

Table IV. Statistics of the second calibration

	Position error (m) Max	Average	Position error /voyage distance	Time before navigation (s)
Before compensation	115.6	62.7	9.6%	300
After compensation	9.1	5.5	0.8%	300

Fig. 7 and Table IV show the navigation results of the second calibration. We manually added 5 deg of misalignment mounting angles to this calibration. The compensation effect is more obvious in this calibration. The final position error reaches 115 m before compensation. And the max error after compensation is only 9.1 m which equals to 0.8% of the voyage distance.

6 Conclusion

This paper proposed a new approach to solve the mounting angle calibration problem in Doppler sensors aided underwater navigation. By separately treating the body frame and the navigation frame attitude update, the new algorithm could be carried out during the SINS attitude alignment stage that an accurate attitude is still not available. Simulation and experiment results show that the new algorithm could effectively identify the misalignment mounting angles and misalignment attitude in 300 s. It means that the calibration and SINS attitude alignment could be performed simultaneously. And the position errors during the navigation is less than 0.8% of the voyage distance.

Acknowledgments

This work is supported by the National High-tech Research and Development Program of China (2013AA09A414).

DOI: 10.1587/elex.11.20140994
Received October 17, 2014
Accepted November 7, 2014
Publicized November 21, 2014
Copyedited December 10, 2014